Collagen-Silver Nanowire Composites as Electrically Active and Antibacterial Scaffolds for Embryonic Cardiac Cell Proliferation

Abeni Wickham[1], Mikhail Vagin[2], Hazem Khalaf[3], Sergio Bertazzo[5], Peter Hodder[4], Staffan Dånmark[1], Torbjörn Bengtsson[3], Jordi Altimiras[6], Daniel Aili[1]*

[1]Division of Molecular Physics, Department of Physics, Chemistry and Biology (IFM), Linköping University SE- 581 83 Linköping, Sweden. [2]Division of Chemical and Optical Sensor Systems, Department of Physics, Chemistry and Biology (IFM), Linköping University, SE- 581 83 Linköping, Sweden. [3]Faculty of Medicine and Health, School of Health and Medical Sciences, Örebro University, SE-701 82 Örebro, Sweden. [4]TA Instruments Ltd. 730-740 Centennial Court, Centennial Way, Elstree WD6 3SZ, UK, [5]Department of Materials, Imperial College London, London   SW7 2AZ, UK. [6]Division of Biology, Department of Physics, Chemistry and Biology (IFM), Linköping University SE- 581 83 Linköping, Sweden.

ABSTRACT

Electroactive biomaterials are used in a number of applications, including scaffolds for neural and cardiac regeneration. Most electrodes and conductive scaffolds for tissue regeneration are based on synthetic materials that have limited biocompatibility and often display a large mismatch in mechanical properties with the surrounding tissue. In this work we have developed a nanocomposite material prepared from self-assembled collagen and silver nanowires (AgNW) that display electrical properties analogous to electrodes used in the clinic. The AgNW concentration of the nanocomposites was optimized to stimulate proliferation of isolated embryonic cardiomyocytes. In addition, the AgNWs renders the nanocomposites antimicrobial against both Gram-negative *Escherichia coli* and Gram-positive *Staphylococcus epidermidis*. The mechanical properties of the nanocomposites were further characterized in physiological conditions and showed a dynamic modulus within the lower kPa range, suitable for embryonic cardiomyocyte proliferation. An in depth electrochemical analysis of the materials in the wet state showed a charge storage capacity of 12.28 mC cm^{-2}, and charge injection capacity of 0.33 mC cm^{-2}, comparable to electrode materials, such as iridium oxide and polypyrrole, currently used for electrical stimulation of tissues. The collagen/AgNW composites are thus multifunctional structural scaffolds that promote embryonic cardiomyocyte function, with the ability to store and inject charges, along with providing antimicrobial resistance.

1. Introduction

The clinical need for restoring damaged, lost, or dysfunctional tissues is not met by the available amount of donor tissues and organs. Synthetic polymers have been extensively scrutinized as temporary support for regenerating tissues and in some cases as permanent replacements.[1] A significant difference between materials developed for replacing and regenerating tissues, lies in the ability to combine tissue specific mechanical and structural properties with biological cues for better integration of implants and regeneration of surrounding tissue.[2] Electrically active scaffolds have been shown to promote cellular electrotaxis in wound healing[3], regeneration of nerve tissue[4], and have more recently been applied for cardiac regeneration.[5,6] Specifically, for myocardial regeneration after infarct, the necessity of retaining and promoting electrical coupling between the cells that drive the pulsatile motion of the heart has become a key engineering challenge.[7] Consequently, there has been extensive research focused on the development of electrically active materials based on, e.g. conjugated polymers with high charge storage capacity.[8] Coating of critical nerve gaps with poly(3,4-ethylenedioxthiophene) (PEDOT) to increase the conduction velocity and thus regeneration in rats has been shown to be effective in the short-term.[9] However, PEDOT and other conjugated polymers, including polypyrrole and polyaniline, are non-biodegradable and brittle.[10] In certain tissues, such as the heart, conjugated polymers could cause adverse immune responses upon implantation, as the ischemic myocardium is a hostile environment where inflammatory responses can perpetuate the scarring.[11].

Another approach to make conductive materials mechanically match soft tissue, is to incorporate inorganic nanoparticles and nanowires in hydrogels. Auguste et al. showed that spherical gold nanoparticles (AuNPs) could be synthesized in a HEMA-based scaffold, leading to an increase in

conductivity of the materials.[12] Silicone field effective transistors embedded in Matrigel and synthetic scaffolds has also been shown to be conductive enough to enable real time monitoring of electrochemical signals from cardiomyocytes and neural cells.[13] Most of these systems, however ingenious, require complicated fabrication procedures and use of materials that are not yet approved for medical implants.

Collagen is one of the main structural components of the extracellular matrices.[14] Collagen in different forms can be found from the cornea to bones, where it is usually associated with other structural proteins and glycosaminoglycans. In some tissues, the collagen interacts with inorganic components, e.g. in bone, the collagen fibril growth is initiated and oriented by hydroxyapatite nanoparticles.[15] *In vitro*, the collagen self-assembly, folding and fibrillation process can be simulated using collagen molecules redissolved in dilute acidic conditions.[16] When the pH of the collagen solution is increased within a high salt environment, it initiates nucleation of the molecules.[17] Fibril growth rapidly commences once the solution is heated to 37°C. Plastic compression of collagen, a technique for making collagen meshes, utilizes fibril reassembly to make tissue-like constructs mimicking the *in vivo* extracellular matrix (ECM).[18,19] Collagen on its own in not conductive, and has consequently limited capabilities in electrical stimulation of cells. The introduction of conductive components to a collagen system would hence allow for a biomimetic material that could improve stimulation, regeneration and remodeling of tissues relying on electrical stimulation.

Silver in the form of nanoparticles has played a large role in consumer products for years.[20] High concentrations of silver nanowires (AgNWs) embedded in polydimethylsiloxane has previously been shown to result in highly conductive and stretchable materials.[21] In addition to being conductive, silver (Ag) nanoparticles (AgNPs) have also been extensively used in antimicrobial

coatings in medical devices such as stents, and wound care products, as it can also be safely cleared out the body.[22,23]

In this work, we have developed biocompatible nanocomposites by homogenously incorporating AgNWs in fibrous collagen meshes prepared through plastic compression. The nanocomposites show an appropriate biocompatibility, antimicrobial activity, and charge injection capacity for the use as an electrically active biomaterial. The effect of varying concentrations of AgNWs in the nanocomposite on the proliferation of embryonic chicken cardiomyocytes was investigated. The materials with highest cell viability were further characterized for their rheological fingerprint, in physiological conditions. Hydrated conductivity measurements in the form of charge storage/injection capacity of the materials were also investigated, along with its antimicrobial activity against both Gram-negative and Gram-positive bacteria. These initial studies show that the collagen/AgNW composite is a multifaceted material for electrical stimulation that also inhibits bacterial growth, for future use in tissue regeneration. In the case of electrodes for direct stimulation of the cells with good interfacing contacts, the collagen/AgNW composite is comparable to metallic and conjugated polymer systems, with the added functionalities of tissue mimetic composition, nanostructure and mechanical properties as well as cell compatibility.

2. Materials and Methods

2.1 Preparation of collagen/AgNW composites

A modified plastic compression procedure based on the technique developed by Brown et al. was used.[24] Briefly, lyophilized, rat-tail collagen (First Link, UK) was dissolved in 0.1 mM acetic acid at a concentration of 5 mg/ml. Minimum essential medium, MEM (First Link, UK) was added to the solution in a dilution of 1:10, MEM:collagen. The pH was then incrementally raised from 2 to 7 with 5 N NaOH. The solution was kept on ice for 10 minutes before addition of different concentrations of silver nanowires with an average diameter 90 nm and length 30 µm, dissolved in water (Blue Nano, USA). The suspensions were then incubated for 20 minutes at 37°C, before being compressed using 200µm spaced nylon and stainless steel meshes. The materials were kept in 1X phosphate buffered saline for storage.

2.2 Scanning electron microscopy (SEM) and Energy-dispersive X-ray spectroscopy (EDS)

Samples were dried using increasing concentrations of ethanol in water and finally in hexamethyldisilazane (HMDS) for 15 minutes. These samples were then sputter coated with 10 nm platinum (Leica EM SCD 500) and then imaged at an accelerating voltage of 5 kV (Leo 1550 Gemini, Zeiss, Germany). EDS was carried out using 80mm^2 X-Max Silicon Drift Detector and the AztecEnergy software (Oxford Instruments). The elemental analysis were collected in the form of a map together with the electron microscopy image and spectra, with an accelerating voltage of 20 kV and working distance of 8.5 mm for all samples. Density-dependent color scanning electron microscopy (DDC-SEM) imaging was performed with the composites attached to a sample holder, which was then coated with 10 nm chromium (Quorum Technologies Sputter

Coater model K575X). The composites were imaged by SEM (Gemini 1525 FEGSEM), operating at 10 kV. The DDC-SEM images were obtained by imaging a region in backscatter mode and subsequently imaging the same region in the inlens mode. With the ImageJ software, images were stacked and the inlens image was assigned to the green channel whereas the backscatter image was assigned to the red channel.

2.3 Cell isolation and proliferation assays

Isolation of cardiomyocytes was done with the approval from the Linköping Ethical Committee (Dnr. 9-13). Fertilized Ross 308 broiler eggs were obtained from a hatchery (Lantmännen Swehatch, Väderstad, Sweden) and incubated at a temperature of 37.8°C, with a relative humidity of 45% and 21% oxygen, for 19 days. The embryonic chicken cardiomyocytes (ECCM) were harvested by decapitating the 19 day old embryos, and collecting whole hearts into Tyrode's buffer (pH 7.35, 5 mM KCl, 10 mM glucose, 140 mM NaCl, 1 mM $MgCl_2$, 10 mM HEPES) kept at 4°C. The atria were cleaved and removed. The ventricles were minced and exposed to enzymatic degradation with 120 U/ml collagenase and 0.525 U/ml protease for 10 minutes at 37°C. The supernatant of the enzymatic solution was collected up to 10 repeats and centrifuged for 5 minutes at 300 g. The pellet was suspended in Tyrode's buffer supplemented with 200 µM Ca^{2+} and kept on ice. The aliquots were then pooled, centrifuged and the pellets resuspended in Tyrode's with 400 µM Ca^{2+}. The cells were pre-plated in cell culture media with 1 mM Ca^{2+} for 1.5 hours to reduce contamination from endothelial cells and fibroblasts. The cardiomyocytes remaining in solution were then centrifuged, counted and plated in flasks and left in an incubator kept at 37°C, 5% CO_2 for two days before seeding on the materials.

The materials were cut with a 6 mm trephine, to fit into the 96 well plates. The samples were cleaned overnight in 3X penicillin/streptomycin in sterile PBS at 4°C. Just before cell seeding the samples were rinsed thrice with PBS. The ECCM were seeded at a density of 10^4 cell/well in supplemented DMEM (10%FBS, 1% Essential Amino Acids, 1% Sodium Pyruvate and 1% penicillin/streptomycin). Cell proliferation rates were tested using the 3-(4,5-dimethylthiazol-2-yl)-5-(3-carboxymethoxyphenyl)-2-(4-sulfophenyl)-2H-tetrazolium, inner salt (MTS) assay (CellTiter96® Aqueous one solution, Promega, Madison, WI). Here, the materials were placed into a new well and the media was changed to starvation DMEM (with 0 % FBS). Then 20 µL of MTS assay was added to each well. The absorbance was read at 490 nm (ASYS UVM240 microplate reader). At the same time intervals, a Live/Dead assay was performed by using Live/Dead® Viability/Cytotoxicity Kit (Life Technologies, CA, USA). The materials were imaged at each time point with a confocal fluorescence microscope (Zeiss LSM 700). SEM imaging was done on samples at the same time points using the aforementioned technique.

2.4 Antimicrobial studies

Escherichia coli MG1655 and *Staphylococcus epidermidis* were grown on Luria-Bertani (LB)-agar plates overnight at 37º C. Single colonies were inoculated into 5 ml LB broth and the tubes were incubated at 37º C overnight on shaker set at 200 rpm. Bacterial suspension was inoculated into 5 ml LB broth or spread (100 µl) onto LB-agar plates. The nanocomposites were cut into 6 mm in diameter pieces and placed into the tubes and onto the LB plates. Bacterial growth was monitored over time by measuring the optical density at 620 nm (Multiskan Ascent, Thermo Labsystems) and by microscopically studying the colony density (Olympus CKX41 microscope coupled with Olympus SC30 camera).

2.5 Rheology

Rheological properties of the nanocomposites were investigated using the TA Instruments

Discovery Hybrid Rheometer DHR-3, an 8 mm stainless steel parallel plate and standard Peltier

plate as the temperature module, controlling the temperature isothermally at 37°C. Due to the

hydrophilic nature of the sample, tests were performed using the immersion cell with the sample

immersed in phosphate buffered saline, pH 7.4. In a series of oscillatory experiments, an

amplitude and frequency sweep were used to investigate the strength and frequency dependency

of the viscoelastic properties of the samples, whilst a step transient creep test was performed to

investigate creep ringing. A small controlled axial force was used to provide a slight positive

"loading / pressure" to the top of the sample to ensure good contact.

2.6 Electrochemical characterization

Screen-printed graphite disk electrodes (SPE), diameter 1.8 mm, were obtained from Rusens

LTD (Moscow, Russia). Collagen/AgNW meshes were made with the electrodes incorporated

during incubation at 37°C and then compressed as mentioned above. An Autolab type III

potentiostat (Autolab, EcoChemie, Netherlands) was employed for voltammetric and

amperometric measurements. A saturated calomel electrode (SCE) (Radiometer, Copenhagen)

and a platinum wire were used as the reference electrode and counter electrode, respectively.

The Anson equation (eq. 1) was utilized for the analysis of chronocoulometry data:

$$Q = nFAC\sqrt{\frac{Dt}{\pi}}$$
(eq. 1)

where Q is the charge (C), n the number of electrons transferred in single reaction, F the Faraday

constant (96487 C mol^{-1}), A the surface area (cm^2), C the concentration of substance undergoing

electrode process (M), D the diffusion coefficient (cm^2 s^{-1}) and t the time (s). Electrochemical

impedance spectroscopy (EIS) was carried out in a 10 mM potassium ferricyanide and 10 mM potassium ferrocyanide 0.1 M KCl solution at an applied potential of 0.22 V (versus Ag/AgCl) from 0.1 to 10^5 Hz with a voltage amplitude of 10 mV.

2.7 Statistical analysis

Statistical analysis on MTS results was done using multiple comparisons two-way ANOVA, *post hoc* Tukey's test, with GraphPad Prism (La Jolla CA, USA). Statistical significance was assigned at $p < 0.05$ and are indicated with an asterisk (*). In some instances p values < 0.0001 were calculated and are indicated with (****). P values > 0.05 were denoted as not significant and labeled as 'ns'.

3. Results and Discussion

3.1 Materials Synthesis and Characterization

Collagen gels were prepared by plastic compression of rat-tail type I collagen at a concentration of 5 mg/ml, which resulted in well-defined collagen fibers and a fibrous mesh. Collagen fibril formation was initiated by raising the pH of collagen dissolved in dilute acetic acid to pH 7. After gelation at 37°C a mechanical load was applied while allowing controlled release of water from the collagen gel using capillary flow into a filter.[25]

Figure 1. Optical images of a) Control, 0 mg/ml, b) 0.1 mg/ml, c) 0.5 mg/ml, d) 1 mg/ml, and e) 5 mg/ml collagen/AgNW nanocomposites. Scale bar: 6 mm.

Collagen/AgNW nanocomposites were obtained by introducing AgNWs to the collagen solution just after the nucleation of collagen fibrils, i.e. after increasing the pH to 7. Samples were made with 0.1, 0.5, 1 and 5 mg/ml AgNWs with respect to the initial collagen volume. Fibrous meshes were obtained for all concentrations of AgNWs tested (Figure 1). The resulting nanocomposite meshes had a distinctive silver appearance at the highest AgNW concentrations after compression (Figure 1c-e). The dimensions of the AgNWs used here were on average 90 nm in diameter and 30 μm in length (Figure S1, Supporting Information), which is similar to the size of the collagen fibrils (Figure S2, Supporting Information). The addition of nanowires during fibril formation of the collagen ensured formation of collagen meshes with homogenously dispersed nanowires throughout the material. Additionally, the length of the AgNWs would facilitate

formation of a conductive network even when the NWs are significantly diluted in the collagen matrix. SEM imaging did not reveal any differences in collagen fibril morphology or appearance of the compressed collagen network after addition of AgNWs (Figure S2, Supporting Information). DDC-SEM in conjunction with SEM enabled the distinction between the AgNWs (orange) and the collagen fibrils (green) in Figure 2. Increasing the concentrations of AgNW resulted in a denser network of NWs in the nanocomposites but without formation of any visible aggregates.
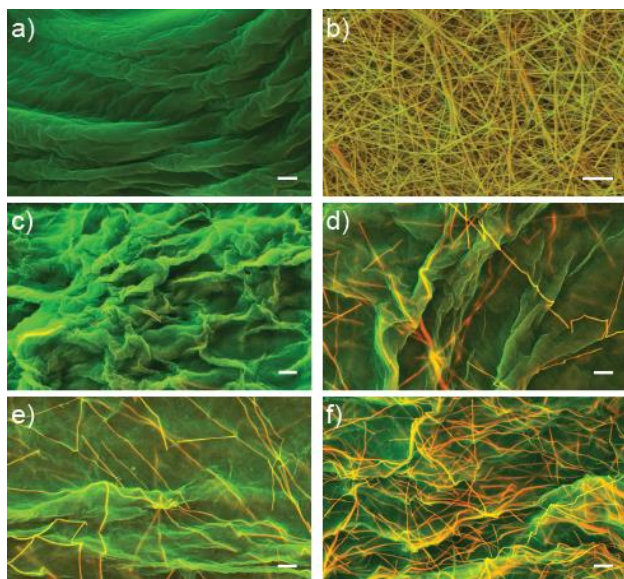

Figure 2. DDC-SEM micrographs of a) collagen after plastic compression (green), b) AgNWs (yellow), and collagen/AgNWs nanocomposites with c) 0.1 mg/ml, d) 0.5 mg/ml, e) 1 mg/ml, f) 5 mg/ml AgNW embedded in collagen. Scale bars: 2 µm.

Electron dispersive X-ray spectroscopy (EDS) was utilized to confirm the presence and distribution of AgNWs in the compressed collagen. The EDS spectra (Figure S3, Supporting Information) show large comparative increases of Ag with the increasing concentrations of Ag, as expected with the exception of the sample with 0.1 mg/ml AgNWs, which only showed a

marginal increase from the control indicated by the presence of Ag Lα1 in the EDS spectrum (Figure S3 inset, Supporting Information).

3.2 Biocompatibility evaluation

The addition of metal nanoparticles/nanowires to insulating but biocompatible polymers can potentially affect cell viability.[26] Therefore, optimization of nanowire concentrations was important to find conditions that would not affect cell proliferation. As an initial evaluation of the effect of AgNW concentrations on cell proliferation, we carried out Live/Dead Cytotoxicity and MTS colorimetric proliferation assays of embryonic chicken cardiomyocytes (ECCMs) cultured on the developed collagen/AgNW nanocomposites. SEM imaging was used at the same time points to further characterize effects on the materials and cell morphology. Freshly isolated ECCM were chosen as a suitable model as their proliferation capacity has been shown to be highly influenced by the material's mechanical and morphological properties.[27-29]

The cells were seeded on the nanocomposites with a density of 10^4 cells/well, where the bottom of the wells was covered by a circular piece of the materials. The cells were assessed for seven days. The addition of AgNWs did affect the proliferation rate of the cells, and the samples with the highest concentrations (0.5 and 1 mg/ml) showed a reduced proliferation as compared to the collagen control (0 mg/mL AgNWs) (Figure 3a). When normalized to the day 7 controls, all samples retained a statistically similar proliferation capacity up to day 5, with the exception that the proliferation was significantly higher on samples with 0.1 mg/ml compared to the control at day 3 $p < 0.05$. However, the higher concentrations of AgNWs (0.5 and 1 mg/ml), reached their highest point of proliferation at day 5, and by day 7 there were significantly fewer cells than on

materials with 0.1 mg/ml AgNWs and the control p < 0.001. There was no significant difference at day 7 between either the control and 0.1 mg/ml or between the 0.5 mg/ml and 1 mg/ml concentrations. The Live/Dead assay showed a similar trend (Figure 3b). There were hardly any dead cells, noted by the lack of red emission of the ethidium homodimer-1.
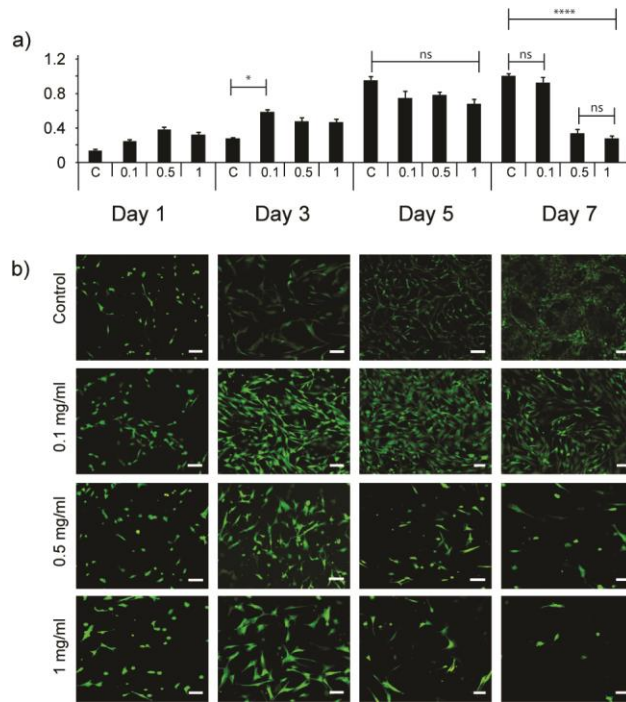

Figure 3. a) MTS assay showing the proliferation of embryonic cardiomyocytes on nanocomposites with different concentrations of AgNWs from Day 1 to 7. The data is normalized with respect to the day 7 collagen control samples. There was a significant lag in growth on the control sample at day 3 (p < 0.05). By day 5, all samples had no statistically significant difference, but on day 7 the 0.5 and 1 mg/ml significantly dropped in cell numbers (p < 0.0001). The 0.1 mg/ml samples were not statistically significantly different from the control samples in the cell proliferation on day 7. b) Live/Dead imaging of ECCMs on nanocomposites with different concentrations of AgNWs. Scale bars: 10 μm.

This lack for imaged dead cells is probably due to the presence of polyvinylpyrrolidone (PVP) remaining from the synthesis of the AgNW. PVP is used to promote the anisotropic growth of the silver into AgNWs and also supports their colloidal stability.[30] Although PVP has been shown to increase biocompatibility of silver nanowires for alveolar epithelial cells.[31] PVP is also known to hinder cell adhesion.[32] Proliferation of cardiomyocytes depends on their proximity to each other, as their survival is reliant on the formation of interconnected networks formed at higher seeding densities.[29] As some cells possibly detached after day 5, there was not a sufficient cell density to promote proliferation on the higher concentrations of collagen/AgNW nanocomposites, seen in the day 7 overview images of the material (Figure S4, Supporting Information). This is further confirmed in the SEM images where the cells are rounded and detaching from the areas with high concentrations of AgNWs (Figure 4).
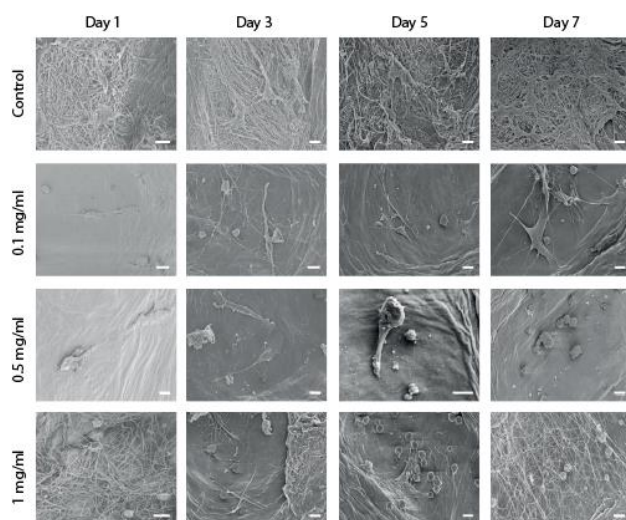

Figure 4. Scanning electron microscopy of embryonic cardiomyocytes cells on collagen (0 mg/mL AgNWs) and collagen/AgNW nanocomposites. Increasing concentrations of AgNWs resulted in rounded and detached cells. The 0, 0.1, and 0.5 mg/ml AgNW samples showed cells with extended morphologies indicative of adhesion. Scale bar: 10 μm

Protrusions of filopodia were seen on the collagen control as well as on nanocomposites with 0.1 and 0.5 mg/ml AgNWs. Rounded cells were found where there were locally high densities of AgNWs, which likely reduced possible attachment sites for the cells (Figure 4). The lowest concentration of AgNW (0.1 mg/ml) showed no significant difference in cell proliferation as compared to the pure collagen control. This concentration was thus found optimal for the continuation of studies, and could be potentially easy to translate into clinical applications as it is a lower concentration than current commercialized nano-silver containing products.[33]

3.3 Antibacterial Properties

Silver has been used for many decades as a powerful antimicrobial agent in hospital settings,[34] and has been used to treat and prevent infections at least since the 1920s.[35] Today, silver in different forms is used in many consumer products to prevent microbial growth.[20] The bactericidal effects of silver and silver nanoparticles is thought to be an effect of direct damage to the cell membranes, disruption of ATP production and DNA replication, and generation of reactive oxygen species (ROS).[36]

The antimicrobial effects of the collagen/AgNW nanocomposite were investigated against Gram-negative *Escherichia coli* and Gram-positive *Staphylococcus epidermidis* bacteria using the standard agar plate test and broth assay. For both bacterial strains, growth inhibition only occurred at the surfaces of the nanocomposites and not in suspension. Meshes with AgNWs were found to suppress *E. coli* and *S. epidermidis* (Figure 5) growth on Luria-Bertani (LB) plates, as indicated by the zones of inhibition. The growth on LB plates was completely suppressed by surfaces containing the highest concentrations of AgNWs (1 and 5 mg/ml). Furthermore, the

meshes without AgNWs were almost completely covered by bacterial colonies after 72 hours (Figure 5). With increasing concentration of AgNWs the zone of inhibition increased. Inhibition of bacterial growth is of large importance for implants of any kind, as some patients do show rejection of whole organ implants due to secondary bacterial infection.[37,38] No inhibition of bacterial growth was seen in solution using the broth assay (Figure S5, Supporting Information), strongly indicating limited leakage of silver from the materials.
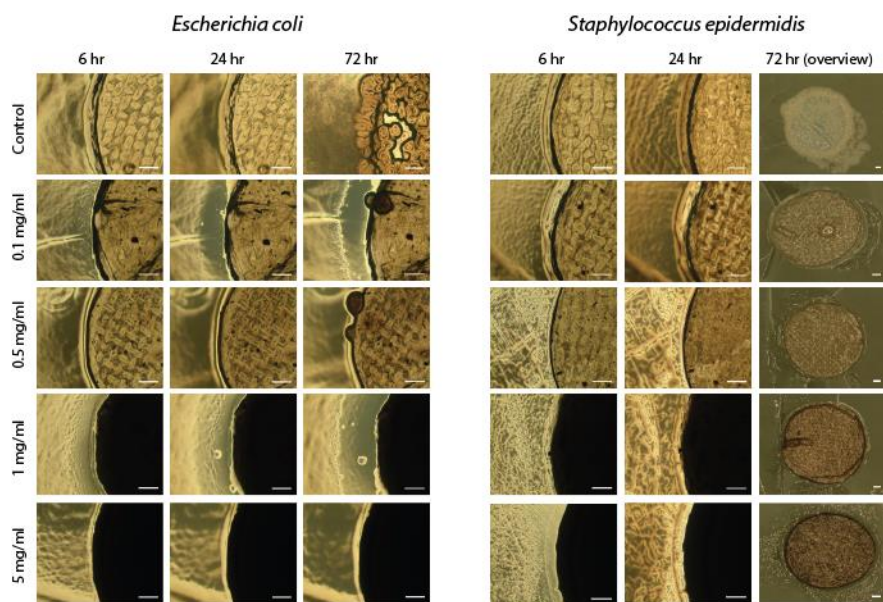

Figure 5. *E. coli and S. epidermidis* spreading on collagen/AgNW nanocomposites from 6 to 72 hours. As the concentration of AgNW increased so did the inhibition to bacterial growth on or near the material. Scale bar: 500 µm.

3.4 Rheology

Rheology was used to explore the influence of AgNWs on the mechanical properties of the collagen meshes. Collagen will deform like a solid until there is a relaxation of the deformation,

where the fluid-like behaviors are indicative of molecular rearrangements.[39] The materials were immersed in PBS buffer (pH 7.4) at 37°C during the measurements, since dehydration of the collagen would significantly alter the mechanical properties of the nanocomposites.[40] Small differences in thickness and swelling characteristics of each sample were accounted for by applying a small controlled axial force to provide a slight positive pressure to the top of the sample, which ensured a good contact (Figure S6, Supporting Information). A series of oscillatory experiments, and amplitude and frequency sweeps were used to investigate the strength and frequency dependency of the viscoelastic properties of the samples.

All samples showed frequency independency for a wide frequency range, suggesting gel like network structures (Figure S7, Supporting Information). The addition of AgNWs had a small effect on the storage modulus (G') of the materials, though; it did affect the loss modulus (G'') significantly (Figure 6a). The nanocomposites with 0.5 mg/ml AgNWs showed higher G' values and lower G'' values than materials with 0.1 mg/ml AgNWs, and significantly lower G'' than collagen only meshes, suggesting that the AgNW contributions make the materials more rigid. With increasing torques there was a significant increase in G'' in samples with 0.5 mg/ml AgNWs, indicating that the interactions between AgNWs and collagen were disrupted resulting in more fluid-like behavior.

A step transient creep test was performed to investigate creep ringing of the material, which can show differences in rigidity (Figure 6b). The amplitude of the ringing was different for all the materials. Materials with 0.5 mg/ml AgNWs showed lower amplitudes and dampened faster than the pure collagen (control) meshes, whereas materials with 0.1 mg/ml AgNWs showed the opposite. The AgNWs consequently seem to disrupt the collagen network and at the lowest concentration (0.1 mg/ml) of AgNWs, the NWs were too dispersed to reinforce the material. In

the materials with 0.5 mg/ml AgNWs, on the other hand, the density of the AgNWs was high enough to reinforce the collagen network. This was further confirmed by the higher G' and lower G'' values for nanocomposites with 0.5 mg/mL AgNWs as compared to materials with 0.1 mg/mL AgNWs. (Figure 6a).
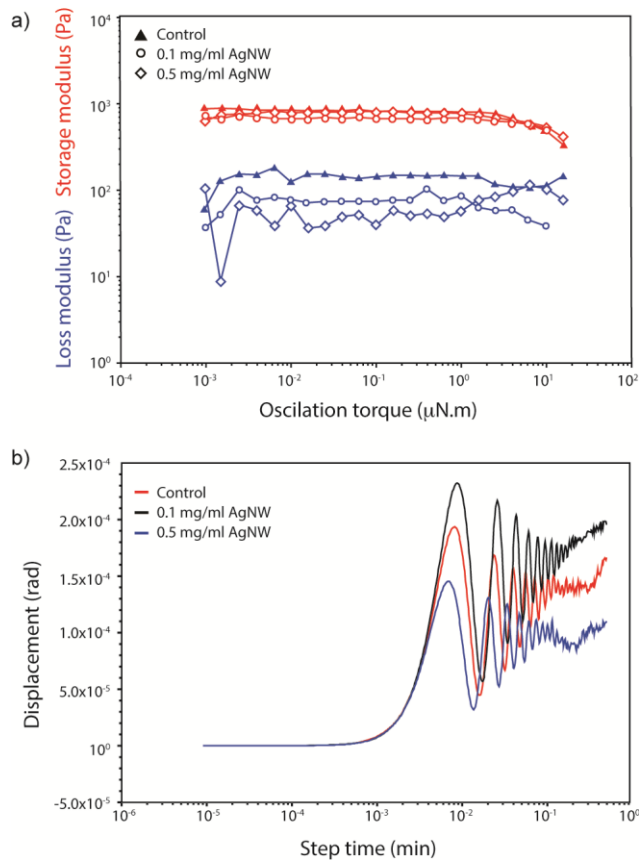

Figure 6. a) Amplitude sweeps showing the storage modulus (G') and loss modulus (G''), and b) step transient creep ringing of collagen meshes and collagen/AgNW nanocomposites with 0 (control), 0.1 and 0.5 mg/ml AgNWs.

Soft gels with G' values around 1 kPa have been shown to efficiently support and produce beating cardiomyocytes,[28] and these nanocomposites are in the same range. In addition, the relatively high concentration of collagen (5 mg/ml) used for the preparation of the

collagen/AgNW nanocomposites allows for a more sturdy material apt for suturing as compared to the much softer collagen meshes resulting from lower collagen concentrations normally used (2-3 mg/ml).[18,41]

3.5 Electrochemical properties

The dried collagen/AgNW nanocomposites with 5 mg/ml of AgNWs showed a sheet resistance of 600-500 Ω/cm^2, clearly showing that the NWs form a continuous conducting network. The nanocomposites with lower concentrations of AgNWs showed significantly higher sheet resistance values that could not be measured properly with a four-point probe. Since the ability to inject and store charges in the wet state are the most important property of the material, the electrochemical properties of the nanocomposites were evaluated by inserting screen-printed graphite disk electrodes into the collagen/AgNW nanocomposites before the onset of the gelation, i.e. before incubation at 37°C. Electrochemical impedance spectroscopy (EIS) measurements of the biocompatible nanocomposites in faradaic processing conditions using ferro/ferricyanide as a redox probe, revealed an increase in the electrode reaction rate in the presence of AgNWs (Figure S8, Supporting Information). The impedance spectrum of nanocomposites with 0.1 mg/mL AgNWs showed a higher frequency arc of a smaller diameter than the collagen only materials (0 mg/mL AgNWs), caused by the heterogeneous electron transfer of the redox probe electrode reaction. A Randles equivalent circuit (Figure S8 inset, Supporting Information) was used to quantitatively characterize the effect. This equivalent circuit consisted of a double layer capacitance (C_{DL}) in series with a solution resistance (R_S) and in parallel with a diffusional branch, i.e. charge transfer resistance (R_{CT}) and Warburg impedance

(W). Fitting of the EIS experimental spectra (Table 1) showed 1.35 times lower value of R_{CT} obtained at 0.1 mg/ml collagen/AgNW in comparison with collagen alone, which illustrates the increase of the electrode reaction rate of the ferro/ferricyanide couple in the presence of AgNWs. A 1.4 times larger double layer capacitance and a 1.6 times smaller Warburg coefficient was observed for the collagen/AgNW nanocomposite in comparison to the collagen alone. This is a likely consequence of the presence of the AgNWs, which would increase the electrode surface area and specific double layer capacitance.
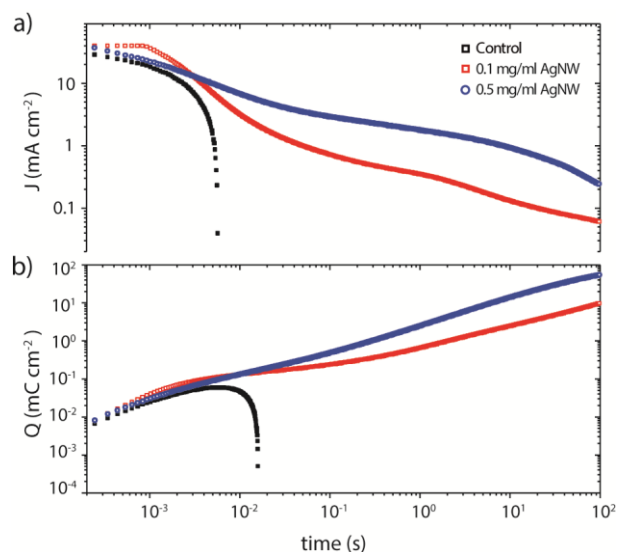

Figure 7. Charge injection properties of collagen, 0.1 and 0.5 mg/ml collagen/AgNW nanocomposites. The transients of (**a**) current and, (**b**) charge densities, obtained at 0.6 V pulse with pure collagen (■) and collagen/AgNW composites (0.1 mg/ml (□) and 0.5 mg/ml (○) AgNW).

Table 1. Fitted parameters of a Randles equivalent circuit, R$_S$, the solution resistance C$_{DL}$ the double layered capacitance, R$_{CT}$ the charge transfer resistance, and Warburg impedance.

Parameter		0 mg/ml	0.1mg/ml
RS	[□]	184	151
CDL	[□F]	8.7	12.3
RCT	[□]	308	228
W	[k□ s-$^{0.5}$]	2.5	1.6

Cyclic voltammetry (CV) showed an apparent current increase at both cathodic and anodic regions with the presence of AgNWs (Figure S9, Supporting Information). However, the contributions of Ag redox reactions could not be readily resolved with this technique, presumably because the AgNWs are both capped with polyvinylpyrrolidone (PVP) and embedded in the dense collagen mesh.

As the nanocomposites were expected to store electrical charges and be able to excite cells surrounding it, the faradaic charge storage capacity was investigated using chronoamperometry in a wide domain of sampling times. The measurements were carried out under conditions suitable for cell stimulation using the inherent redox-activity of the embedded AgNW, i.e. no additional redox active species were added. A long potential pulse from the regions of low (0 V) to high currents (0.6 V) was applied to the materials. The recorded transient current densities showed a significant change in the characteristics for the nanocomposites as compared to the collagen only meshes (Figure 7a and Figure S10, Supporting Information). The pure collagen samples (0 mg/mL AgNWs) showed lower currents with a fast decay whilst the 0.1, and 0.5

mg/ml collagen/AgNW nanocomposites revealed dramatically slower decays of currents characterized by slopes close to -0.5 in double logarithmic coordinates. This illustrates the Cottrell's current decay due to the influence of the electrode reaction by planar diffusion, where the increase in AgNW concentration led to higher currents.

Transients of surface-normalized integral charge (Figure 7b) showed that the collagen/AgNW nanocomposites have a charge storage capacity that increased with time, reaching values of 2.3 mC cm^{-2} and 12.28 mC cm^{-2} at the 10 s pulse for AgNW concentrations of 0.1 mg/ml and 0.5 mg/ml, respectively. These values are close to the best reported for optimized electrode materials for neural stimulation, such as iridium oxide, 28.8 mC cm^{-2} [42], polypyrrole, 48.8 mC cm^{-2},[43] poly (3,4 ethylenedioxythiophene), 75.6 mC cm^{-2},[44,45] and an order of magnitude higher than platinum in pacemakers, 208 µC/cm^2.[46] The charge injection capacity, i.e. the amount of charges that can move through the electrodes, characterized at shorter times reached a value of 0.33 mC cm^{-2} and 0.94 mC cm^{-2} at a pulse time of 300 ms for 0.1 mg/ml and 0.5 mg/ml collagen/AgNW, respectively. As a comparison, this is similar to the charge injection capacity reported for polypyrrole-based neural electrodes (1.17 mC) developed for electrical stimulation of skeletal muscles.[43]

The Anson plot was used for the linearization of the obtained charge transients (Figure S11, Supporting Information). Assuming the concentration of substance undergoing electrode process is equal to metallic silver one can calculate the apparent diffusion coefficients of Ag ions inside the collagen composites: 1×10^{-10} cm^2 s^{-1} and 0.7×10^{-10} cm^2 s^{-1} for the 0.1 mg/ml and 0.5 mg/ml collagen/AgNW composites, respectively. These values are small enough to illustrate the efficient entrapment of the AgNWs within the collagen nanocomposite, which ensures that there

is no leakage of Ag ions. This was also confirmed from the lack of inhibition of bacterial growth bacterial growth in solution using the broth assay.

The embryonic cardiomyocytes showed no difference in proliferation based on the conductive properties of the AgNW content in the 0.1 mg/ml nanocomposites. However, cardiomyocytes cultured on conductive AuNP/HEMA hydrogels have been shown to increase the connexin 43 (Cx43) expression, both with and without electrical stimulation, as compared to materials without AuNPs.[12] A similar observation was made by Kohane et al. showing that cardiomyocytes cultured on alginate scaffolds impregnated with gold nanowires (AuNWs) enhances Cx43 expression without stimulation. The presence of AuNWs lead to a significant increase in the amount of Cx43 and α-sarcomeric actinin as compared to when cultured on pristine alginate scaffolds.[47] This suggests that metal nanoparticles embedded in a biocompatible scaffold, indeed, can impart phenotypic traits in cultured cardiomyocytes that can improve the function of engineered cardiac tissue.

Conclusions

Here we show the development of collagen/silver nanowire (AgNW) nanocomposites that are simple to fabricate but offer multiple functionalities in addition to mimicking the multi-scale structural complexity of the extracellular matrix. The nanocomposites are mainly consist of fibrillar collagen and behave as soft gels with a storage modulus of about 1 kPa, but display charge storage/injection capacities in the similar orders of magnitude as notable electrode materials like platinum and iridium oxide. The lowest concentration of AgNW (0.1 mg/ml) showed no significant difference in proliferation of freshly isolated embryonic cardiac cell as

compared to the pure collagen control, whereas higher concentrations of AgNWs lead to a reduction in proliferation. The antimicrobial capacity of the nanocomposites provides the possibility for long lasting storage and reduced need for antibiotics in the clinical setting. The scaffolds described here, thus present a new approach to easily fabricate soft biomaterial scaffolds for tissue engineering applications benefitting from efficient electrical stimulation.

Supplementary Information: SEM of AgNWs and collagen/AgNW nanocomposites, EDS spectra of collagen/AgNW nanocomposites, Live/Dead images of ECCMs on collagen/AgNW nanocomposites, data on bacterial broth assay, additional rheology and electrochemical data. This material is available free of charge via the Internet at http://pubs.acs.org.

AUTHOR INFORMATION

Corresponding Author

*Daniel Aili

Division of Molecular Physics, Department of Physics, Chemistry and Biology (IFM), Linköping University SE- 581 83 Linköping, Sweden. Email: daniel.aili@liu.se

Author Contributions

A.W. designed the study, performed sample preparations, cell isolations, biocompatibility studies, SEM, data interpretation, and prepared the manuscript. M.V. carried out electrochemical analysis and interpretation. H.K carried out antimicrobial studies. S.B evaluated samples with

DDC-SEM method. P.H. carried out rheology and data interpretation. S.D aided with defining the study and manuscript preparation. T.B supervised antimicrobial studies. J.A provided embryonic chicken eggs and supervised cell isolations and manuscript revisions. D.A. supervised the study, aided with study design, data interpretation and revisions of manuscript.

REFERENCES

(1)   Nair, L. S.; Laurencin, C. T. Biodegradable Polymers as Biomaterials. *Prog. Polym. Sci.* 2007, *32*, 762–798. DOI:10.1016/j.progpolymsci.2007.05.017

(2)   Hronik-Tupaj, M.; Kaplan, D. L. A Review of the Responses of Two- and Three-Dimensional Engineered Tissues to Electric Fields. *Tissue Eng., Part B* 2012, *18*, 1–14. DOI:10.1089/ten.teb.2011.0244

(3)   Kloth, L. C. Electrical Stimulation for Wound Healing: a Review of Evidence From in Vitro Studies, Animal Experiments, and Clinical Trials. *IJLEW* 2005, *4*, 23–44. DOI: 10.1177/1534734605275733

(4) Fabbro, A.; Sucapane, A.; Toma, F. M.; Calura, E.; Rizzetto, L.; Carrieri, C.; Roncaglia, P.; Martinelli, V.; Scaini, D.; Masten, L.; Turco, A.; Gustincich, S.; Prato, M.; Ballerini, L. Adhesion to Carbon Nanotube Conductive Scaffolds Forces Action-Potential Appearance in Immature Rat Spinal Neurons. *PLoS ONE* 2013, *8*, e73621–14. DOI: 10.1371/journal.pone.0073621.

(5) Zimmermann, W.-H.; Melnychenko, I.; Wasmeier, G.; Didié, M.; Naito, H.; Nixdorff, U.; Hess, A.; Budinsky, L.; Brune, K.; Michaelis, B.; Dhein, S.; Schwoerer, A.; Ehmke, H.; Eschenhagen, T. Engineered Heart Tissue Grafts Improve Systolic and Diastolic Function in Infarcted Rat Hearts. *Nat. Med.* 2006, *12*, 452–458. DOI:10.1038/nm1394

(6) Tandon, N.; Cannizzaro, C.; Chao, P.-H. G.; Maidhof, R.; Marsano, A.; Au, H. T. H.; Radisic, M.; Vunjak-Novakovic, G. Electrical Stimulation Systems for Cardiac Tissue Engineering. *Nat. Protoc.* 2009, *4*, 155–173. DOI: 10.1038/nprot.2008.183.

(7) Vunjak-Novakovic, G.; Lui, K. O.; Tandon, N.; Chien, K. R. Bioengineering Heart Muscle: a Paradigm for Regenerative Medicine. *Annu. Rev. Biomed. Eng.* 2012, 245–267. DOI: 10.1146/annurev-bioeng-071910-124701.

(8) Guo, L.; Ma, M.; Zhang, N.; Langer, R.; Anderson, D. G. Stretchable Polymeric Multielectrode Array for Conformal Neural Interfacing. *Adv. Mater.* 2013, *26*, 1427–1433. 10.1002/adma.201304140

(9) Egeland, B. M.; Urbanchek, M. G.; Peramo, A.; Richardson-Burns, S. M.; Martin, D. C.; Kipke, D. R.; Kuzon, W. M., Jr.; Cederna, P. S. In Vivo Electrical Conductivity Across Critical Nerve Gaps Using Poly(3,4-Ethylenedioxythiophene)-Coated Neural Interfaces. *Plast. Reconstr. Surg.* 2010, *126*, 1865–1873. DOI: 10.1097/PRS.0b013e3181f61848.

(10) Cogan, S. F.; Plante, T. D.; Ehrlich, J. Sputtered Iridium Oxide Films (SIROFs) for Low-Impedance Neural Stimulation and Recording Electrodes. Conf. Proc. IEEE, Eng. Med Biol. Soc. 2004; Vol. 4, pp 4153–4156. DOI: 10.1109/IEMBS.2004.1404158

(11) Nahrendorf, M.; Pittet, M. J.; Swirski, F. K. Monocytes: Protagonists of Infarct Inflammation and Repair After Myocardial Infarction. *Circulation* 2010, *121*, 2437–2445. DOI: 10.1161/CIRCULATIONAHA.109.916346

(12) You, J.-O.; Rafat, M.; Ye, G. J. C.; Auguste, D. T. Nanoengineering the Heart: Conductive Scaffolds Enhance Connexin 43 Expression. *Nano Lett.* 2011, *11*, 3643–3648. DOI: 10.1021/nl201514a.

(13) Tian, B.; Liu, J.; Dvir, T.; Jin, L.; Tsui, J. H.; Qing, Q.; Suo, Z.; Langer, R.; Kohane, D. S.; Lieber, C. M. Macroporous Nanowire Nanoelectronic Scaffolds for Synthetic Tissues. *Nat Mater* 2012, *11*, 1–9. DOI:10.1038/nmat3404

(14) Brodsky, B.; Persikov, A. V. Molecular Structure of the Collagen Triple Helix. *Adv. Protein Chem.* 2005, *70*, 301–339. DOI:10.1016/S0065-3233(05)70009-7

(15) Wang, Y.; Azaïs, T.; Robin, M.; Vallée, A.; Catania, C.; Legriel, P.; Pehau-Arnaudet, G.; Babonneau, F.; Giraud-Guillem MM.; Nassif N. The Predominant Role of Collagen in the Nucleation, Growth, Structure, and Orientation of Bone Apatite. *Nat. Mater.* 2012, *11*, 724–733. DOI: 10.1038/nmat3362.

(16) Holmes, D. F.; Capaldi, M. J.; Chapman, J. A. Reconstitution of Collagen Fibrils: the assembly process depends on the initiating procedure *Int. J. Biol. Macromol.* 1986, *8*, 161–166. DOI:10.1016/0141-8130(86)90020-6

(17) Kuznetsova, N.; Leikin, S. Does the Triple Helical Domain of Type I Collagen Encode Molecular Recognition and Fiber Assembly While Telopeptides Serve as Catalytic Domains?: Effect of proteolytic cleavage on fibrillogenesis and on collagen-collagen interaction in fibers. *J. Biol. Chem.* 1999, *274*, 36083–36088. DOI: 10.1074/jbc.274.51.36083

(18) Levis, H. J.; Brown, R. A.; Daniels, J. T. Plastic Compressed Collagen as a Biomimetic Substrate for Human Limbal Epithelial Cell Culture. *Biomaterials* 2010, *31*, 7726–7737. DOI: 10.1016/j.biomaterials.2010.07.012.

(19) Cheema, U.; Brown, R. A. Rapid Fabrication of Living Tissue Models by Collagen Plastic Compression: Understanding Three-Dimensional Cell Matrix Repair in Vitro. *Adv. Wound Care* 2013, *2*, 176–184. DOI: 10.1089/wound.2012.0392

(20) Varner, K.; El-Badawy, A.; Feldhake, D.; Venkatapathy, R. State of the Science Literature Review: Everything Nano silver and More. U.S. E.P.A, Washington, DC, EPA/600/R-10/084, 2010, 1–221.

(21) Xu, F.; Zhu, Y. Highly Conductive and Stretchable Silver Nanowire Conductors. *Adv. Mater.* 2012, *24*, 5117–5122. DOI: 10.1002/adma.201201886

(22) Marambio-Jones, C.; Hoek, E. M. V. A Review of the Antibacterial Effects of Silver Nanomaterials and Potential Implications for Human Health and the Environment. *J Nanopart Res* 2010, *12*, 1531–1551. DOI 10.1007/s11051-010-9900-y

(23) Wilkinson, L. J.; White, R. J.; Chipman, J. K. Silver and Nanoparticles of Silver in Wound Dressings: a Review of Efficacy and Safety. *J. Wound Care* 2011, *20*, 543–549.

(24) Brown, L. Cardiac Extracellular Matrix: a Dynamic Entity. *Am. J. Physiol.: Heart Circ. Physiol.* 2005, *289*, H973–H974. DOI: 10.1152/ajpheart.00443.2005

(25) Brown, R. A.; Wiseman, M.; Chuo, C.-B.; Cheema, U.; Nazhat, S. N. Ultrarapid Engineering of Biomimetic Materials and Tissues: Fabrication of Nano- and Microstructures by Plastic Compression. *Adv. Funct. Mater.* 2005, 1762–1770. DOI: 10.1002/adfm.200500042

(26) Schinwald, A.; Chernova, T.; Donaldson, K. Use of Silver Nanowires to Determine Thresholds for Fibre Length-Dependent Pulmonary Inflammation and Inhibition of Macrophage Migration in Vitro. *Part. Fibre Toxicol.* 2012, *9*, 1–1. DOI:10.1186/1743-8977-9-47

(27) Laflamme, M. A.; Gold, J.; Xu, C.; Hassanipour, M.; Rosler, E.; Police, S.; Muskheli, V.; Murry, C. E. Formation of Human Myocardium in the Rat Heart From Human Embryonic Stem Cells. *Am. J. Pathol.* 2005, *167,* 663–671. DOI: http://dx.DOI.org/10.1016/S0002-9440(10)62041-X

(28) Engler, A. J.; Carag-Krieger, C.; Johnson, C. P.; Raab, M.; Tang, H. Y.; Speicher, D. W.; Sanger, J. W.; Sanger, J. M.; Discher, D. E. Embryonic Cardiomyocytes Beat Best on a Matrix with Heart-Like Elasticity: Scar-Like Rigidity Inhibits Beating. *J. Cell Sci.* 2008, *121*, 3794–3802. DOI: 10.1242/jcs.029678.

(29) Madden, L. R.; Mortisen, D. J.; Sussman, E. M.; Dupras, S. K.; Fugate, J. A.; Cuy, J. L.; Hauch, K. D.; Laflamme, M. A.; Murry, C. E.; Ratner, B. D. Proangiogenic Scaffolds as Functional Templates for Cardiac Tissue Engineering. *Proc. Natl. Acad. Sci. U.S.A.* 2010, *107,* 15211–15216. DOI: 10.1073/pnas.1006442107

(30) Sun, Y.; Mayers, B.; Herricks, T.; Xia, Y. Polyol Synthesis of Uniform Silver Nanowires: a Plausible Growth Mechanism and the Supporting Evidence. *Nano Lett.* 2003, *3*, 955–960. DOI: 10.1021/nl034312m

(31) Stoehr, L. C.; Gonzalez, E.; Stampfl, A.; Casals, E.; Duschl, A.; Puntes, V.; Oostingh, G. J. Shape Matters: Effects of Silver Nanospheres and Wires on Human Alveolar Epithelial Cells. *Part. Fibre Toxicol.* 2011, *8*, 36. DOI:10.1186/1743-8977-8-36

(32) Gorfu, G.; Virtanen, I.; Hukkanen, M.; Lehto, V. P.; Rousselle, P.; Kenne, E.; Lindbom, L.; Kramer, R.; Tryggvason, K.; Patarroyo, M. Laminin Isoforms of Lymph Nodes and Predominant Role of 5-Laminin(S) in Adhesion and Migration of Blood Lymphocytes. *J. Leukocyte Biol.* 2008, *84*, 701–712. DOI:10.1189/jlb.0108048

(33) Benn, T. M.; Westerhoff, P. Nanoparticle Silver Released Into Water From Commercially Available Sock Fabrics. *Environ. Sci. Technol.* 2008, *42*, 4133–4139. DOI: 10.1021/es7032718

(34) Drake, P. L. Exposure-Related Health Effects of Silver and Silver Compounds: a Review. *Ann. Occup. Hyg.* 2005, *49*, 575–585. DOI: 10.1093/annhyg/mei019

(35) Kissmeyer, A. Some Biological Considerations in the Treatment of Gonorrhea, and Their Practical Application. *Br. J. Vener. Dis.* 1928, *4*, 199–204.

(36) Li, W.-R.; Xie, X.-B.; Shi, Q.-S.; Zeng, H.-Y.; OU-Yang, Y.-S.; Chen, Y.-B. Antibacterial Activity and Mechanism of Silver Nanoparticles on Escherichia Coli. *Appl. Microbiol. Biotechnol*. 2009, *85*, 1115–1122. DOI: 10.1007/s00253-009-2159-5.

(37) Chong, A. S.; Alegre, M-L. The Impact of Infection and Tissue Damage in Solid-Organ Transplantation. *Nat. Rev. Immunol.* 2012, *12*, 459–471. DOI: 10.1038/nri3215.

(38) Busscher, H. J.; van der Mei, H. C.; Subbiahdoss, G.; Jutte, P. C.; van den Dungen, J. J. A. M.; Zaat, S. A. J.; Schultz, M. J.; Grainger, D. W. Biomaterial-Associated Infection: Locating the Finish Line in the Race for the Surface. *Sci. Transl. Med.* 2012, *4*, 153rv10–153rv10. DOI: 10.1126/scitranslmed.3004528

(39) Shayegan, M.; Forde, N. R. Microrheological Characterization of Collagen Systems: From Molecular Solutions to Fibrillar Gels. *PLoS ONE* 2013, *8*, e70590. DOI: 10.1371/journal.pone.0070590

(40) Masic, A.; Bertinetti, L.; Schuetz, R.; Chang, S.-W.; Metzger, T. H.; Buehler, M. J.; Fratzl, P. Osmotic Pressure Induced Tensile Forces in Tendon Collagen. *Nat. Commun.* 2014, *6*, 1–8. DOI:10.1038/ncomms6942

(41) Ghezzi, C. E.; Muja, N.; Marelli, B.; Nazhat, S. N. Real Time Responses of Fibroblasts to Plastically Compressed Fibrillar Collagen Hydrogels. *Biomaterials* 2011, 4761–4772. DOI: 10.1016/j.biomaterials.2011.03.043.

(42) Cogan, S. F. Neural Stimulation and Recording Electrodes. *Ann. Rev. Biomed. Eng.* 2008, *10*, 275–309. DOI: 10.1146/annurev.bioeng.10.061807.160518

(43) Guo, L.; Ma, M.; Zhang, N.; Langer, R.; Anderson, D. G. Stretchable Polymeric Multielectrode Array for Conformal Neural Interfacing. *Adv. Mater.* 2014, *26*, 1427–1433. DOI: 10.1002/adma.201304140

(44) Wilks, S. Poly(3,4-Ethylene Dioxythiophene) (PEDOT) as a Micro-Neural Interface Material for Electrostimulation. *Front. Neuroeng.* 2009, *2*, 1-8. DOI: 10.3389/neuro.16.007.2009

(45) Venkatraman, S.; Hendricks, J.; King, Z. A.; Sereno, A. J.; Richardson-Burns, S.; Martin, D.; Carmena, J. M. In Vitro and in Vivo Evaluation of PEDOT Microelectrodes for Neural Stimulation and Recording. *IEEE Trans. Neural Syst. Rehabil. Eng.* 2011, *19*, 307–316. DOI: 10.1109/TNSRE.2011.2109399

(46) Norlin, A.; Pan, J.; Leygraf, C. Investigation of Electrochemical Behavior of Stimulation/Sensing Materials for Pacemaker Electrode Applications. *J. Electrochem. Soc.* 2005, *152*, J7. DOI: 10.1149/1.1842092

(47) Dvir, T.; Timko, B. P.; Brigham, M. D.; Naik, S. R.; Karajanagi, S. S.; Levy, O.; Jin, H.; Parker, K. K.; Langer, R.; Kohane, D. S. Nanowired Three-Dimensional Cardiac Patches. *Nat. Nanotechnol.* 2011, 1–6. DOI:10.1038/nnano.2011.160

Table of Contents Graphic and Synopsis.

A collagenous silver nanowire scaffold with electrical charge injection and storage capacities similar to platinum and iridium oxide electrodes but with mechanical properties suitable for embryonic cardiac cell proliferation and antimicrobial resistance is developed.